Theory of superflow in two-dimensional states of ^{3}He in an arbitrary potential well

1992 J. Phys.: Condens. Matter 4 9531

(http://iopscience.iop.org/0953-8984/4/48/009)

J. Phys.: Condens. Matter 4 (1992) 9531–9544. Printed in the UK

Theory of superflow in two-dimensional states of ^{3}He in an arbitrary potential well

Grzegorz Harań and Lucjan Jacak

Institute of Physics, Wrocław University of Technology, Wybrzeże Wyspiańskiego 27, 50-370 Wrocław, Poland

Received 5 May 1992

Abstract. Two-dimensional superfluid states of ^{3}He are studied within a microscopic model, including the effects of the substrate potential and the superflow. The energetic stability of these states is analysed. The phase transition temperature and the critical superflow are found and compared with experiment. The effect of substrate coating with ^{4}He is discussed.

1. Introduction

Progress in experimental low-temperature techniques during the last few years has allowed several groups [1–7] to obtain superfluid ^{3}He in confined geometries. They reported the existence of superfluid currents in thin films with thickness d approaching the zero-temperature coherence length $\xi_0 \simeq 65$ nm (at $P = 0$ bar) [1–7]. Although experimental efforts have focused on determination of the superfluid density and the critical temperature T_c^F of the superfluid transition, the theoretical description of these phenomena is still not sufficient. There are studies by Fetter and Ullah [8] and Jacobsen and Smith [9] in which the superflow is calculated, but in the Ginzburg–Landau regime only. Some experiments are carried out in a different temperature limit [2] and it is not possible to compare them with these theoretical predictions. In this paper the superfluidity is studied within the microscopic theory and the results obtained are valid for all temperatures. As mentioned in our first paper [10] for the $T = 0$ limit, our aim is to investigate the influence of the substrate potential on the superfluid state. One of the experimental groups [1, 4, 5] reported that both the superflow and the critical temperature depend strongly on the kind of substrate. These two quantities are considerably enhanced when the adsorbent is coated with ^{4}He. Freeman *et al* [6] suggested that ^{4}He atoms smooth out the substrate irregularities and change the scattering of ^{3}He quasiparticles off the wall from diffuse to specular. In our work we want to describe another effect caused by covering the substrate with ^{4}He. We suggest that not only the kind of substrate scattering but also the interaction of ^{3}He quasiparticles with the substrate through the van der Waals forces is weakened by isolating layers of ^{4}He. Using a simple model with a substrate potential we find measurable quantities like the maximal superflow j_{Sc} and the critical temperature T_c^F. We study the two-dimensional states. Therefore, our results are correct for films not thicker than ξ_0, a little thinner than those experimentally accessible now. However, as explained further in the text, our

0953-8984/92/489531+14$07.50

analysis may also be relevant for films with thickness d of the order of the temperature-dependent coherence length $\xi(T)$, especially at low temperatures, which is a limit not covered so far in the literature. The other thickness limit for this model is $d \gg p_0^{-1}$, where $p_0 = (3\pi^2 n)^{1/3}$ is the bulk Fermi momentum and n is the bulk density of ^{3}He. This condition ensures that the interactions between quasiparticles are almost the same as for the bulk system.

In this paper we use the atomic units $\hbar = k_B = 1$.

2. Model

We discuss a thin film of constant thickness d. The z axis is chosen orthogonal to the film surface. This system is approximated by the infinite potential well [11]:

$$V_1(z) = \begin{cases} 0 & \text{for } 0 < z < d \\ \infty & \text{for } z \leqslant 0 \text{ or } z \geqslant d \end{cases}. \tag{2.1}$$

In order to study the influence of the substrate forces on the adsorbed fluid, we add the van der Waals-like field [12]:

$$V_2(z) = \begin{cases} V > 0 & \text{for } 0 \leqslant z \leqslant a \\ 0 & \text{for } z < 0 \text{ or } z > a \end{cases} \tag{2.2}$$

where V and a are the amplitude and the range of the potential, respectively.

The potential modelling the thin film is a superposition of V_1 and V_2:

$$V(z) = V_1(z) + V_2(z). \tag{2.3}$$

This simple potential takes the repulsive part of the substrate field into account, whereas the almost flat long-range attractive part is approximated by the bottom of the well. This approximation is consistent with potentials calculated by means of variational methods [13, 14] and based on the well known Lennard-Jones or Azis formulae. As shown by Krotscheck *et al* [13] ^{4}He layers isolate ^{3}He from the substrate and displace it to the region of a weaker potential. The point in our approximation is to simulate by a step potential the effect of coating the substrate with ^{4}He. Different values of the potential $V_2(z)$ correspond to different ^{4}He coverages of the surface. It should be added that potentials calculated in [13, 14] have rather intricate oscillatory shape and lead to the existence of some surface states. Fortunately, we deal with films of thickness much larger than the interatomic distance ($d \gg p_0^{-1}$) and the number of states substantially exceeds this very limited number of bound states. That is, we can neglect the surface states in a macroscopic effect like superfluidity. The potential $V(z)$ may be treated as the simplified effective mean field acting on the superfluid.

Simple considerations show that the only parameters that characterize the quasiparticle energy spectrum are d/a and V/μ, where μ is the chemical potential of the system. In figures 1 and 2 we show the single-particle energy spectrum ϵ_ν for such a potential and its dependence on the above parameters for fixed μ. From now on this field will be given by two dimensionless parameters d/a and Va^2.

The energy spectrum of that system is

$$\epsilon_\nu(p) = p^2/(2m) + \epsilon_\nu \qquad \nu = 1, \ldots, \nu_c \tag{2.4}$$

where $\nu_c = \max\{\nu : \epsilon_\nu \leqslant \mu\}$, $p = (p_x, p_y)$ is the two-dimensional momentum and m is the mass of the ^{3}He atom. The Fermi momentum of the quantum state number

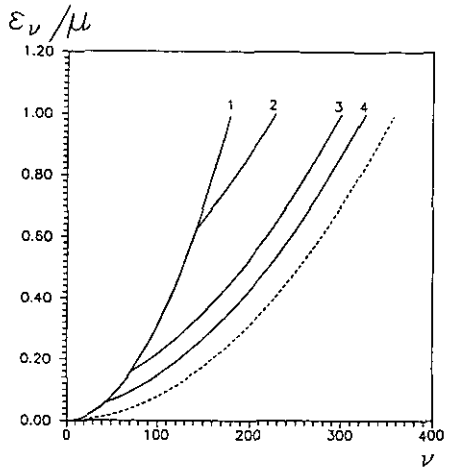

Figure 1. The single-particle energy spectrum for $d/a = 2$ and (1) $2mVa^2 = 90000\pi^2$, (2) $2mVa^2 = 10000\pi^2$, (3) $2mVa^2 = 2500\pi^2$ and (4) $2mVa^2 = 900\pi^2$; the broken curve represents the energy spectrum of the infinite potential well.

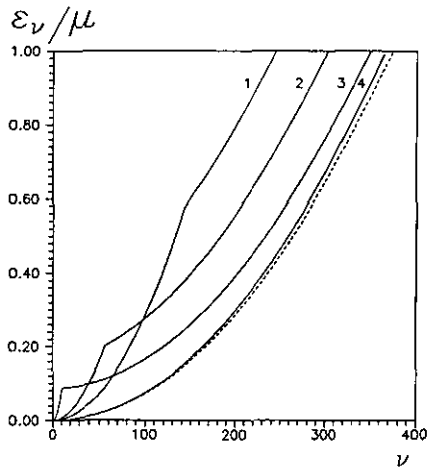

Figure 2. The single-particle energy spectrum for $2mVa^2 = 10000\pi^2$ and (1) $d/a = 2$, (2) $d/a = 1.5$, (3) $d/a = 1.1$ and (4) $d/a = 50$; the broken curve represents the energy spectrum of the infinite potential well.

ν is $p_F \sin\vartheta_\nu$, where $\sin\vartheta_\nu = (1 - \epsilon_\nu/\mu)^{1/2}$. The inclusion of the potential $V_2(z)$ makes the energy levels unequally spaced.

For a given density n, the two-dimensional Fermi momentum p_F and the bulk Fermi momentum $p_0 = (3\pi^2 n)^{1/3}$ are connected by

$$p_F = p_0\left[2p_0 d\left(3\pi\sum_{\nu=1}^{\nu_c}\sin^2\vartheta_\nu\right)^{-1}\right]^{1/2}. \tag{2.5}$$

3. Formalism

We introduce the Matsubara–Green function for a non-interacting system of fermions in a thin film [11, 15]:

$$\mathcal{G}_{0\nu}(i\omega_n, p) = [i\omega_n - \epsilon_\nu(p) + \mu]^{-1} \tag{3.1}$$

where $\omega_n = (2n+1)\pi T$ and $\epsilon_\nu(p)$ is defined by equation (2.4). The Green functions $\mathcal{G}_\nu(i\omega_n, p)$ and $\mathcal{F}_\nu(i\omega_n, p)$ for a superfluid state are determined by the Abrikosov–Gorkov equations [16]:

$$\mathcal{G}_\nu(i\omega_n, p) = \mathcal{G}_{0\nu}(i\omega_n, p) + \mathcal{G}_{0\nu}(i\omega_n, p)\Delta_\nu(p)\mathcal{F}_\nu^+(i\omega_n, p) \tag{3.2}$$

$$\mathcal{F}_\nu^+(i\omega_n, p) = -\mathcal{G}_{0\nu}^-(i\omega_n, p)\Delta_\nu^+(p)\mathcal{G}_\nu(i\omega_n, p). \tag{3.3}$$

The order parameter $\Delta_\nu(p)$ is found from the following self-consistent gap equation:

$$\Delta_\nu^+(p) = -T\sum_{p_1,\nu_1,n} V_{\nu\nu_1}(\hat{p}, \hat{p}_1)\mathcal{F}_{\nu_1}^+(i\omega_n, p_1) \tag{3.4}$$

where

$$V_{\nu\nu_1}(\hat{p},\hat{p}_1)_{\alpha\beta\gamma\delta} = \tfrac{3}{2}g(\hat{p}\hat{p}_1 \sin\vartheta_\nu \sin\vartheta_{\nu_1} + \cos\vartheta_\nu \cos\vartheta_{\nu_1})(\delta_{\alpha\gamma}\delta_{\beta\delta} + \delta_{\alpha\delta}\delta_{\beta\gamma}) \quad (3.5)$$

is the p-pairing interaction for thin films [11, 15], g is the bulk coupling constant and the superscript '–' in equation (3.3) denotes time inversion.

The presence of a superflow in a system is introduced by a Galilean transformation [17, 18]:

$$p \to p + mv \quad (3.6)$$

where v is the superfluid velocity and is assumed to be independent of spatial coordinates. With accuracy to linear terms in v, which is consistent with the assumption that $v \ll p_F/m$, this transformation implies a shift of Matsubara frequencies:

$$i\omega_n \to i\omega_n - v \cdot p. \quad (3.7)$$

Since we have restricted our considerations to films of thickness $d \leqslant \xi_0$, the order parameter $\Delta_\nu(p)$ is not a function of z and superfluidity is two-dimensional. The order parameter will be discussed more thoroughly further in the paper.

4. Transition temperature

The superfluid transition temperature T_c^F [12] is obtained from equations (3.2)–(3.4):

$$T_c^F/T_c^B = (2\omega_c e^\gamma/\pi T_c^B)^X \qquad X = 1 - 2p_0 d\left(3\pi \sum_{\nu=1}^{\nu_c} \sin^2\vartheta_\nu\right)^{-1} \quad (4.1)$$

where T_c^B is the bulk critical temperature and ω_c is the energy cut-off parameter. In calculations we have assumed $\omega_c/T_c^B = 100$ according to appropriate Bardeen–Cooper–Schrieffer (BCS) relations; ω_c should be interpreted as the limiting upper value of definite quasiparticle excitations in a system.

The critical temperature T_c^F as a function of film thickness for some values of potential $V(z)$ is shown in figure 3. There is qualitative agreement between presented relations and experimental results [2, 3]. As seen from figure 3, the van der Waals field substantially reduces T_c^F. This is consistent with the experimental results of Harrison *et al* [1, 4], when different ^{4}He coverages of the surface correspond to different values of the potential $V(z)$. However, it is not possible to fit the measured transition temperature as a function of thickness with a simple $V(z)$ field. The small jumps in theoretically calculated T_c^F (see figure 3) are due to quantum size effects. The similar behaviour of measured T_c^F [2, 3] is of the same origin; however, in some cases it can be associated with experimental errors.

5. Superfluid phases

Now we turn our attention to the order parameter $\Delta_\nu(p)$. Note that both the angular momentum L and the spin S of a pair of quasiparticles are unit vectors. The order parameter $\Delta_\nu(p)$ is represented by the spherical tensors $|J,m\rangle$ [19] with J denoting the total angular momentum of a Cooper pair and m its projection on the z

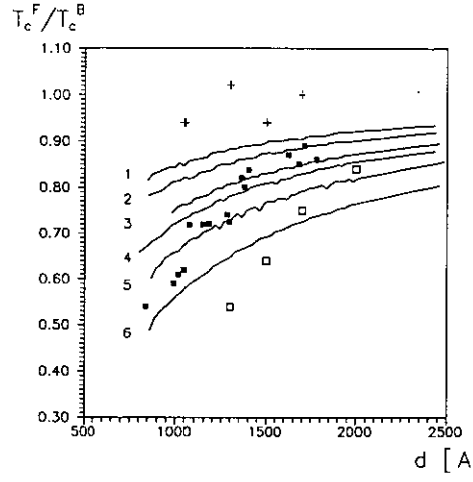

Figure 3. The phase transition temperature T_c^F as a function of film thickness d for several values of substrate field: (1) $d/a = 50$, $2mVa^2 = 2500\pi^2$; (2) $d/a = 40$, $2mVa^2 = 10000\pi^2$; (3) $d/a = 30$, $2mVa^2 = 90000\pi^2$; (4) $d/a = 50$, $2mVa^2 = 100\pi^2$; (5) $d/a = 20$, $2mVa^2 = 100\pi^2$; (6) $d/a = 30$, $2mVa^2 = 100\pi^2$. The results of Xu and Crooker [2] are represented by the full squares and those of Harrison *et al* [1, 4] by the open squares (pure ^{3}He) and the crosses (one ^{4}He layer).

axis. It is obvious that for the two-dimensional momentum p the angular momentum projection m_L attains only two values $m_L = \pm 1$ and simple considerations lead to the representation of $\Delta_\nu(p)$ by six spherical tensors $|J, m\rangle$:

$$\Delta_\nu(p) = \Delta \sin\vartheta_\nu(a_{0,0}|0,0\rangle + a_{1,0}|1,0\rangle + a_{1,1}|1,1\rangle + a_{1,-1}|1,-1\rangle + a_{2,2}|2,2\rangle + a_{2,-2}|2,-2\rangle). \tag{5.1}$$

The order parameter for a p-paired system is conventionally defined as [20]:

$$\Delta_\nu(p) = \Delta(d(\hat{p},\nu)\hat{\sigma})i\sigma_y \tag{5.2}$$

where $\hat{\sigma} = (\sigma_x, \sigma_y, \sigma_z)$ are Pauli matrices. The vector $d(\hat{p},\nu)$ is represented by a tensor d_{ij} [20]:

$$d_i(\hat{p},\nu) = d_{ij}\hat{p}_j \sin\vartheta_\nu. \tag{5.3}$$

Using the explicit form of the tensor $|J, m\rangle$ we can write

$$d_{ij} = (1/\sqrt{3})a_{0,0}\delta_{ij} + (1/\sqrt{2})a_{1,0}(\delta_{iy}\delta_{jx} - \delta_{ix}\delta_{jy}) + (1/2)ia_{1,1}\delta_{iz}(\delta_{jx} + i\delta_{jy}) + (1/2)ia_{1,-1}\delta_{iz}(\delta_{jx} - i\delta_{jy}) + (1/2)a_{2,2}(\delta_{ix} + i\delta_{iy})(\delta_{jx} + i\delta_{jy}) + (1/2)a_{2,-2}(\delta_{ix} - i\delta_{iy})(\delta_{jx} - i\delta_{jy}). \tag{5.4}$$

This general form of the tensor d_{ij} can also be obtained by setting $\hat{p}_z = 0$ in $d(\hat{p})$ for a three-dimensional superfluid [21].

The gap equation (3.4) can be written in a convenient form [19]:

$$d_{ij}\hat{p}_j\sigma_i i\sigma_y = T_{jl}^{ik} d_{kl}\hat{p}'_l\sigma_k i\sigma_y \tag{5.5}$$

where T is the operator acting on the right side of equation (3.4), and the upper and lower indices refer to spin and orbital degrees of freedom respectively. In the absence of a magnetic field the tensor T_{jl}^{ik} is independent of spin indices:

$$T_{jl}^{ik} = T_{jl}\delta_{ik}. \tag{5.6}$$

Then the gap equation (5.5) reduces to

$$d_{ij}\hat{p}_j = T_{jl}d_{il}\hat{p}'_l. \tag{5.7}$$

We obtain two main unitary phases that are invariants of equation (5.7): the two-dimensional A phase (2-A)

$$d_{ij} = \tfrac{1}{2}\mathrm{i}\left[(a_{1,1} + a_{1,-1})\,\delta_{jx} + \mathrm{i}\,(a_{1,1} - a_{1,-1})\,\delta_{jy}\right]\delta_{iz} \tag{5.8}$$

and the two-dimensional B phase (2-B)

$$d_{ij} = [(1/\sqrt{3})a_{0,0}\delta_{jx} - (1/\sqrt{2})a_{1,0}\delta_{jy}]\delta_{ix} + [(1/\sqrt{3})a_{0,0}\delta_{jy} + (1/\sqrt{2})a_{1,0}\delta_{jx}]\delta_{iy}. \tag{5.9}$$

It is convenient to transform these tensors and write the order parameter as

$$d = \begin{pmatrix} 0 & 0 \\ 0 & 0 \\ \Delta_1 & \mathrm{i}\Delta_2 \end{pmatrix} \tag{5.10}$$

$$\Delta_\nu(\boldsymbol{p}) = \sqrt{3/2}\sin\vartheta_\nu(\Delta_1\hat{p}_x + \mathrm{i}\Delta_2\hat{p}_y)\sigma_z\mathrm{i}\sigma_y \tag{5.11}$$

for the 2-A state and

$$d = \begin{pmatrix} \Delta_1 & -\Delta_2 \\ \Delta_2 & \Delta_1 \\ 0 & 0 \end{pmatrix} \tag{5.12}$$

$$\Delta_\nu(\boldsymbol{p}) = \sqrt{3/2}\sin\vartheta_\nu\left[(\Delta_1\hat{p}_x - \Delta_2\hat{p}_y)\sigma_x + (\Delta_2\hat{p}_x + \Delta_1\hat{p}_y)\sigma_y\right]\mathrm{i}\sigma_y \tag{5.13}$$

for the 2-B state.

The amplitudes Δ_1 and Δ_2 are determined by the gap equation (3.4) and are usually different for each phase. The above phases (5.10)–(5.13) are generalizations to the case with broken rotational symmetry of two-dimensional phases obtained by Brusov and Popov [22]. The superflow in the plane of the film breaks the symmetry of the system with respect to rotations about the z axis. However, each phase corresponds to a different quantum number m (the z component of the total angular momentum); namely the 2-A phase corresponds to $m = 1$ whereas the 2-B one is associated with $m = 0$, as in the case of an unbroken rotational symmetry. The first of these phases may also be interpreted as the bulk phase in the proximity of the substrate surface with the angular momentum vector $\boldsymbol{l}$ orthogonal to the surface plane [20, 23, 24]. That is, the superfluid state in films with thickness $d \simeq \xi(T)$ is approximated at low temperature by the two-dimensional A phase (5.10)–(5.11). Also the bulk B phase, due to the orientational wall effects, can be thought of as the two-dimensional B phase (5.12)–(5.13) in the proximity of the surface [25].

It was proved [22] that the 2-A and the 2-B phases are degenerate and stable when there is no flow in the system. The problem of a superfluid current in the Ginzburg–Landau regime for thicker films ($d > \xi(T)$), where the bulk phases occur, was studied by Fetter and Ullah [8].

Next we present results of the microscopic theory for two-dimensional superfluids.

6. The two-dimensional A phase

The gap equation (3.4) for the 2-A phase is

$$\Delta_1 = 3gN_0\frac{\pi}{p_0 d}\Delta_1\sum_{\nu=1}^{\nu_c}\sin^2\vartheta_\nu\int_0^{\omega_c}\mathrm{d}\epsilon\int_0^{\pi/2}\frac{\mathrm{d}\phi}{\pi}\frac{\cos^2\phi}{E_\nu}\left[\tanh\left(\frac{E_\nu^+}{2T}\right)+\tanh\left(\frac{E_\nu^-}{2T}\right)\right] \tag{6.1}$$

$$\Delta_2 = 3gN_0\frac{\pi}{p_0 d}\Delta_2\sum_{\nu=1}^{\nu_c}\sin^2\vartheta_\nu\int_0^{\omega_c}\mathrm{d}\epsilon\int_0^{\pi/2}\frac{\mathrm{d}\phi}{\pi}\frac{\sin^2\phi}{E_\nu}\left[\tanh\left(\frac{E_\nu^+}{2T}\right)+\tanh\left(\frac{E_\nu^-}{2T}\right)\right] \tag{6.2}$$

where

$$E_\nu = \left[\epsilon^2+\tfrac{3}{2}\left(\Delta_1^2\cos^2\phi+\Delta_2^2\sin^2\phi\right)\sin^2\vartheta_\nu\right]^{1/2} \tag{6.3}$$

$$E_\nu^\pm = E_\nu \pm vp_F\sin\vartheta_\nu\cos\phi. \tag{6.4}$$

The solution to equations (6.1) and (6.2) was found numerically and is presented for various temperatures in figure 4. The superfluid gap function for finite flow has two non-degenerate components: the component Δ_2 perpendicular to the flow is enhanced whereas the component Δ_1 parallel to the flow is suppressed. There is a phase transition from the 2-A phase ($\Delta_1 \neq 0$ and $\Delta_2 \neq 0$) to the two-dimensional polar phase ($\Delta_1 = 0$), which is only a special case of the 2-A state (5.10)–(5.11). For sufficiently low temperatures this transition is of first order and can be determined by calculating the free energy $F_S^A(\Delta_1,\Delta_2)$. Let us remark that the gap function plays the role of the order parameter in the system, and the gap equations (6.1)–(6.2) are understood as stationary-type conditions of the free energy $F_S^A(\Delta_1,\Delta_2)$. That is,

$$\frac{\partial}{\partial\Delta_1}F_S^A(\Delta_1,\Delta_2)=0 \qquad \text{and} \qquad \frac{\partial}{\partial\Delta_2}F_S^A(\Delta_1,\Delta_2)=0$$

coincide with equations (6.1) and (6.2) respectively. Hence, the free energy $F_S^A(\Delta_1,\Delta_2)$ of the system can be obtained [17] by integrating the gap equations. If we write equation (6.1) as $f_1(\Delta_1,\Delta_2)=0$ and equation (6.2) as $f_2(\Delta_1,\Delta_2)=0$, then the free energy $F_S^A(\Delta_1,\Delta_2)$ is

$$F_S^A(\Delta_1,\Delta_2)-F_N=\int_0^{\Delta_1}f_1(\Delta_1',\Delta_2)\,\mathrm{d}\Delta_1'+\int_0^{\Delta_2}f_2(0,\Delta_2')\,\mathrm{d}\Delta_2' \tag{6.5}$$

where F_N is the free energy of the normal phase. From equation (6.5) we obtain

$$\begin{aligned}F_S^A(\Delta_1,\Delta_2)-F_N = 3gN_0\frac{\pi}{p_0 d}\sum_{\nu=1}^{\nu_c}\int_0^{\omega_c}\mathrm{d}\epsilon\int_0^{\pi/2}\frac{\mathrm{d}\phi}{\pi}\Bigg\{&(\Delta_1^2\cos^2\phi+\Delta_2^2\sin^2\phi)\\ &\times\frac{1}{E_\nu}\sin^2\vartheta_\nu\left[\tanh\left(\frac{E_\nu^+}{2T}\right)+\tanh\left(\frac{E_\nu^-}{2T}\right)\right]\\ &-\tfrac{4}{3}T\left[\ln\left(\cosh\left(\frac{E_\nu^+}{2T}\right)\right)+\ln\left(\cosh\left(\frac{E_\nu^-}{2T}\right)\right)\right.\\ &-\ln\left(\cosh\left(\frac{\epsilon+vp_F\sin\vartheta_\nu\cos\phi}{2T}\right)\right)\\ &\left.-\ln\left(\cosh\left(\frac{\epsilon-vp_F\sin\vartheta_\nu\cos\phi}{2T}\right)\right)\right]\Bigg\}.\end{aligned} \tag{6.6}$$

For the two-dimensional polar phase (2-P) we have

$$F_S^P(\Delta_2) = F_S^A(\Delta_1 = 0, \Delta_2). \tag{6.7}$$

Phase diagrams calculated from equations (6.6) and (6.7) are shown in figure 5. The transition from the two-dimensional A phase to the normal state is always through the two-dimensional polar phase.

Finally we determine the superflow j_S [17, 18]:

$$j_S = \frac{1}{\mathcal{V}} T \sum_{p,\nu,n} \frac{1}{m}(p + mv)\mathcal{G}_\nu(i\omega_n, p) \tag{6.8}$$

where $\mathcal{V}$ is the volume of the sample. After straightforward algebraic evaluations we find

$$j_S = \frac{1}{(3\pi^2)^{1/3}} n^{2/3} \left\{ vp_0 - \left(p_0 d \sum_{\nu=1}^{\nu_c} \sin^2 \vartheta_\nu / 6\pi \right)^{-1/2} \right.$$
$$\left. \times \sum_{\nu=1}^{\nu_c} \sin^2 \vartheta_\nu \int_0^{\omega_c} d\epsilon \int_0^{\pi/2} \frac{d\phi}{\pi} \cos\phi \left[\tanh\left(\frac{E_\nu^+}{2T}\right) - \tanh\left(\frac{E_\nu^-}{2T}\right) \right] \right\}. \tag{6.9}$$

This equation allows us to draw the superflow j_S as a function of superfluid velocity v (see figure 6). Comparing superflows with phase diagrams (figure 5) we conclude that the maximal superflow j_{Sc} is attained in the 2-A phase. Now it is easy to find the relation between the critical superflow j_{Sc} and the temperature. This function is plotted for different values of potential $V(z)$ in figure 7(*a*) and for a constant potential and varying film thickness in figure 7(*b*). As could be expected the superflow j_{Sc} changes substantially with variations of the substrate field.

Before the eventual comparison of the theoretical results with experimental data, we will discuss the properties of the 2-B phase.

7. The two-dimensional B phase

The gap equation (3.4) for the 2-B phase is

$$\begin{pmatrix} \Delta_1 \\ \Delta_2 \end{pmatrix} = 3gN_0 \frac{\pi}{p_0 d} \begin{pmatrix} \Delta_1 \\ \Delta_2 \end{pmatrix} \sum_{\nu=1}^{\nu_c} \sin^2 \vartheta_\nu$$
$$\times \int_0^{\omega_c} d\epsilon \int_0^{\pi/2} \frac{d\phi}{\pi} \frac{\cos^2\phi}{E_\nu} \left[\tanh\left(\frac{E_\nu^+}{2T}\right) + \tanh\left(\frac{E_\nu^-}{2T}\right) \right] \tag{7.1}$$

$$\begin{pmatrix} \Delta_1 \\ \Delta_2 \end{pmatrix} = 3gN_0 \frac{\pi}{p_0 d} \begin{pmatrix} \Delta_1 \\ \Delta_2 \end{pmatrix} \sum_{\nu=1}^{\nu_c} \sin^2 \vartheta_\nu$$
$$\times \int_0^{\omega_c} d\epsilon \int_0^{\pi/2} \frac{d\phi}{\pi} \frac{\sin^2\phi}{E_\nu} \left[\tanh\left(\frac{E_\nu^+}{2T}\right) + \tanh\left(\frac{E_\nu^-}{2T}\right) \right] \tag{7.2}$$

where

$$E_\nu = \left[\epsilon^2 + \tfrac{3}{2}(\Delta_1^2 + \Delta_2^2) \sin^2 \vartheta_\nu \right]^{1/2} \tag{7.3}$$

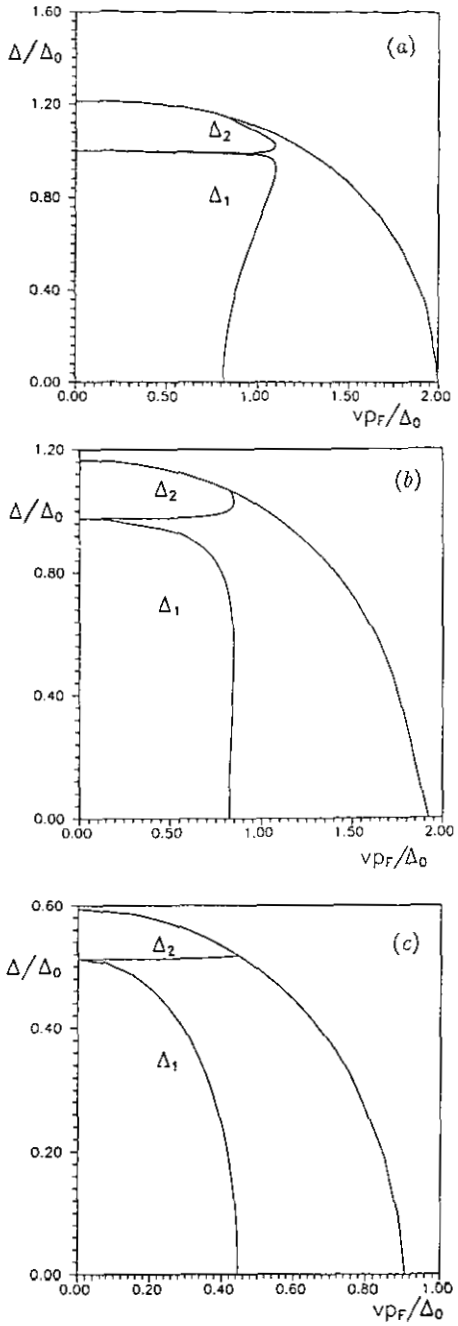

Figure 4. The order parameter as a function of superfluid velocity v for the 2-A phase (full curves) and the 2-P phase (broken curves) at (*a*) $T = 0.1T_c^F$, (*b*) $T = 0.4T_c^F$ and (*c*) $T = 0.9T_c^F$, for the film thickness $p_0d = 100$ and potential constants $d/a = 100$, $2mVa^2 = \pi^2$. $\Delta_0 = \Delta(v = 0, T = 0)$.

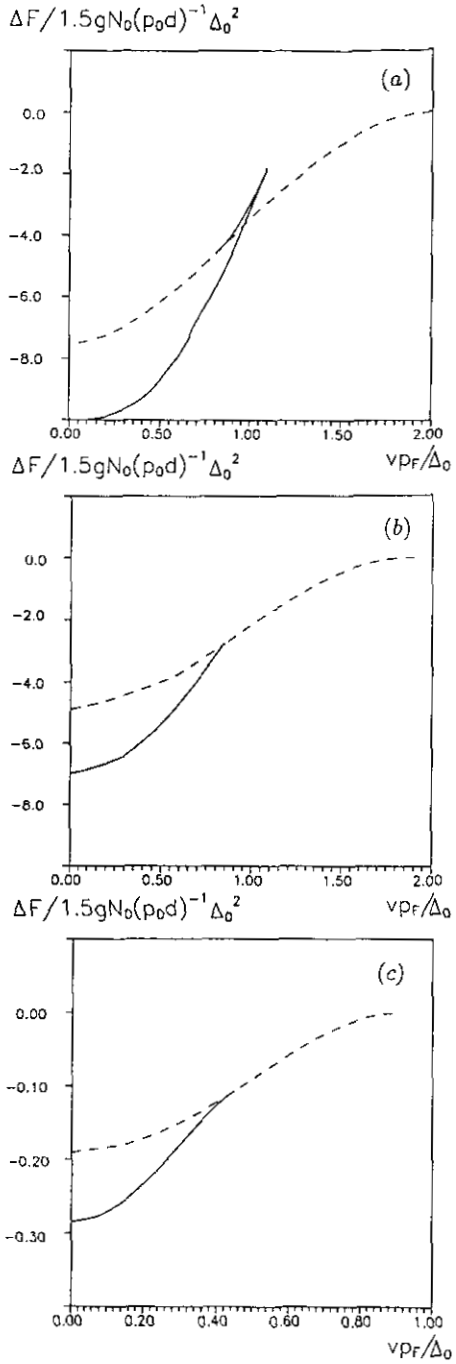

Figure 5. The energy of the 2-A phase (full curves) and the 2-P phase (broken curves) versus the superfluid velocity v at (*a*) $T = 0.1T_c^F$, (*b*) $T = 0.4T_c^F$ and (*c*) $T = 0.9T_c^F$, for the film thickness $p_0d = 100$ and potential constants $d/a = 100$, $2mVa^2 = \pi^2$.

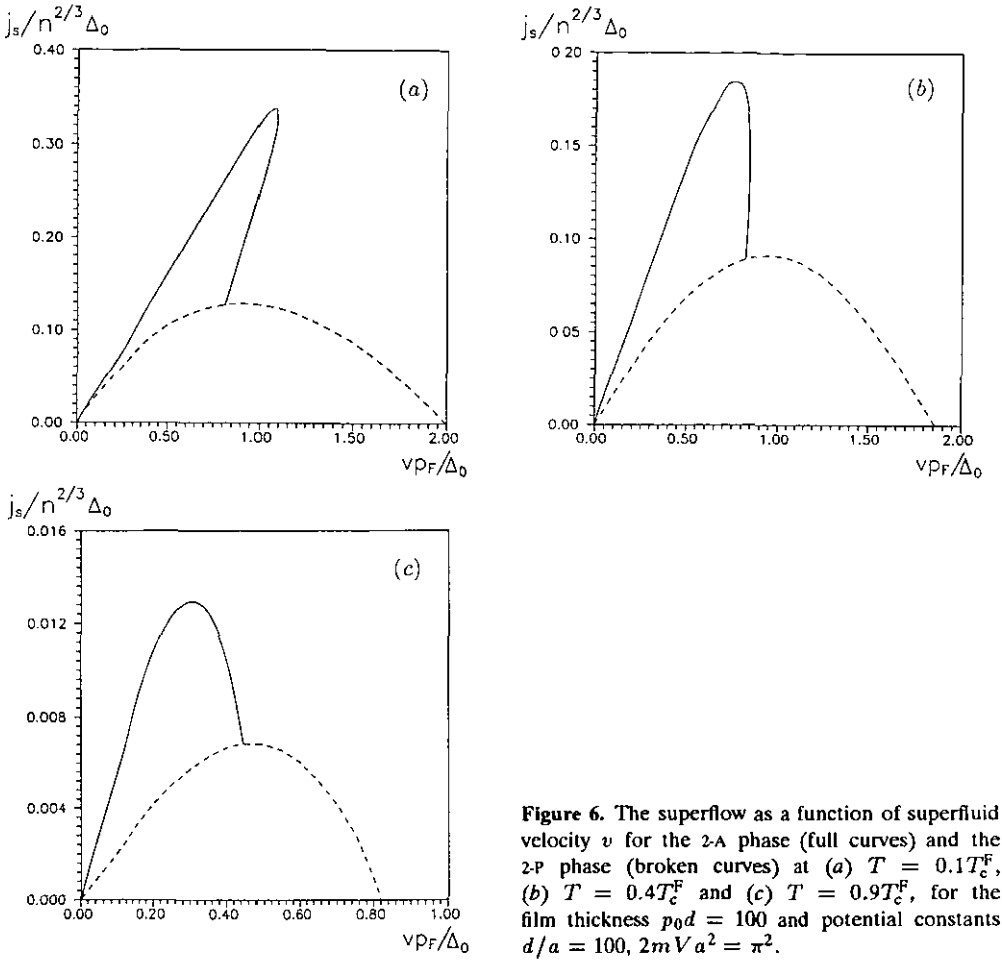

Figure 6. The superflow as a function of superfluid velocity v for the 2-A phase (full curves) and the 2-P phase (broken curves) at (*a*) $T = 0.1T_c^F$, (*b*) $T = 0.4T_c^F$ and (*c*) $T = 0.9T_c^F$, for the film thickness $p_0 d = 100$ and potential constants $d/a = 100$, $2mVa^2 = \pi^2$.

and $E_\nu^\pm$ is defined by equation (6.4). Because this set of equations is invariant under the transformation $\Delta_1 \leftrightarrow \Delta_2$, the only quantity we can determine is $\Delta^2 \equiv \Delta_1^2 + \Delta_2^2$. This is presented for five different temperatures in figure 8; Δ has the interpretation of the magnitude of the order parameter for the 2-B phase.

The methods described in section 5 lead to the formula for free energy:

$$F_S^B(\Delta) - F_N = 3gN_0\frac{\pi}{p_0 d}\sum_{\nu=1}^{\nu_c}\int_0^{\omega_c} d\epsilon \int_0^{\pi/2}\frac{d\phi}{\pi}\left\{\frac{\Delta^2\sin^2\vartheta_\nu}{2E_\nu}\left[\tanh\left(\frac{E_\nu^+}{2T}\right)\right.\right.$$
$$+\tanh\left(\frac{E_\nu^-}{2T}\right)\Big] - \tfrac{4}{3}T\left[\ln\left(\cosh\left(\frac{E_\nu^+}{2T}\right)\right) + \ln\left(\cosh\left(\frac{E_\nu^-}{2T}\right)\right)\right.$$
$$-\ln\left(\cosh\left(\frac{\epsilon + vp_F\sin\vartheta_\nu\cos\phi}{2T}\right)\right)$$
$$\left.\left.-\ln\left(\cosh\left(\frac{\epsilon - vp_F\sin\vartheta_\nu\cos\phi}{2T}\right)\right)\right]\right\}. \tag{7.4}$$

The superflow j_S (6.8) is given by equation (6.9) with E_ν from equation (7.3). From equations (6.9), (7.3) and (7.4) we see that the superflow j_S and the free energy

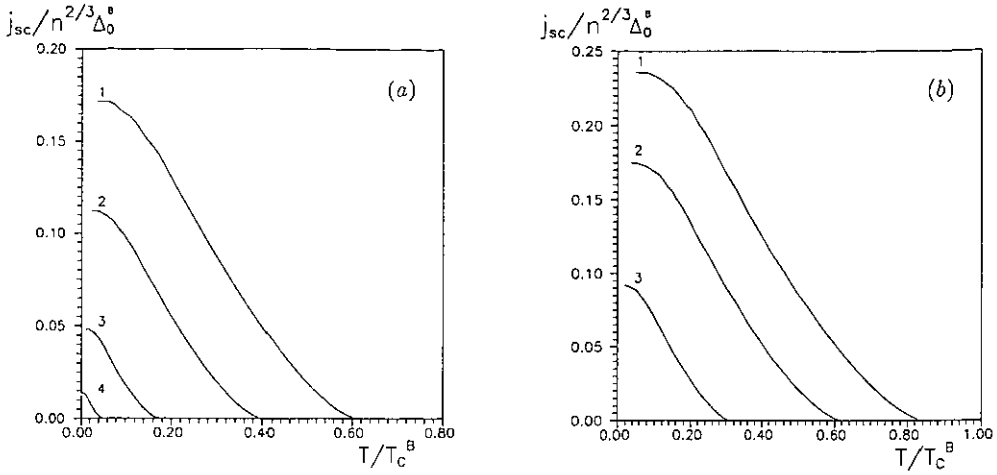

Figure 7. The critical superflow as a function of temperature. (*a*) At a constant film thickness $p_0 d = 100$ and: (1) $d/a = 10$, $2mVa^2 = 100\pi^2$; (2) $d/a = 5$, $2mVa^2 = 400\pi^2$; (3) $d/a = 2.9$, $2mVa^2 = 1225\pi^2$; (4) $d/a = 2$, $2mVa^2 = 2500\pi^2$. (*b*) At a constant potential $2mVa^2 = \pi^2$ and decreasing film thickness: (1) $d/a = 100$, $p_0 d = 100$; (2) $d/a = 25$, $p_0 d = 25$; (3) $d/a = 10$, $p_0 d = 10$. Δ_0^B is the bulk value of the order parameter at $v = 0$ and $T = 0$.

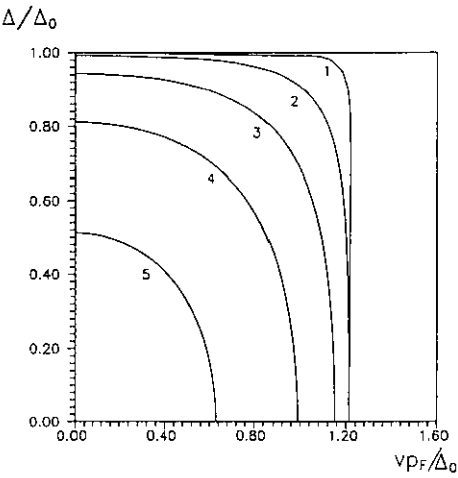

Figure 8. The order parameter for the 2-B phase versus the superfluid velocity v at (1) $T = 0.1T_c^F$, (2) $T = 0.3T_c^F$, (3) $T = 0.5T_c^F$, (4) $T = 0.7T_c^F$ and (5) $T = 0.9T_c^F$, for the film thickness $p_0 d = 100$ and potential constants $d/a = 100$, $2mVa^2 = \pi^2$.

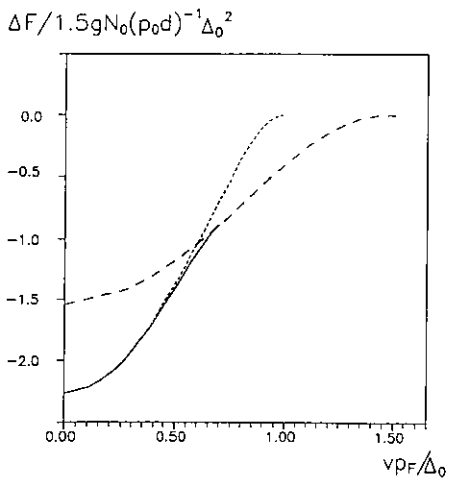

Figure 9. The energy of the 2-B phase (– – –), the 2-A phase (——) and the 2-P phase (— — —) versus the superfluid velocity v at $T = 0.7T_c^F$, for the film thickness $p_0 d = 100$ and potential constants $d/a = 100$, $2mVa^2 = \pi^2$.

$F_S^B(\Delta)$ depend on the gap magnitude Δ only. Comparing equation (6.6) with equation (7.4) one gets $F_S^A(v = 0) = F_S^B(v = 0)$ since at $v = 0$ in both phases $\Delta_1 = \Delta_2$ for symmetry reasons. The degeneracy of these phases is consistent with results of Brusov and Popov [22]. In the presence of a superflow the numerical calculations show the stability of the 2-A phase against the 2-B phase. We present

this result for the temperature $T = 0.7T_c^F$ in figure 9. To complete this analysis the superflow j_S for the two-dimensional B phase is drawn in figure 10.

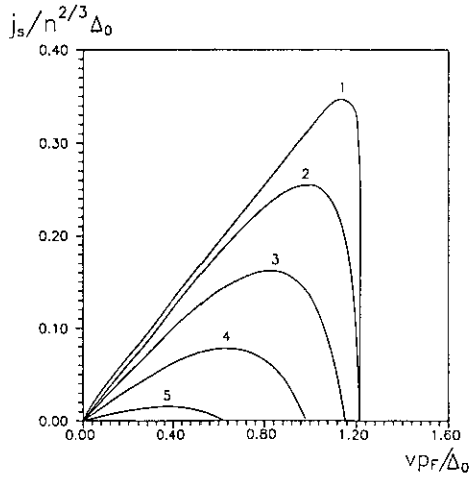

Figure 10. The superflow of the 2-B phase versus the superfluid velocity v at (1) $T = 0.1T_c^F$, (2) $T = 0.3T_c^F$, (3) $T = 0.5T_c^F$, (4) $T = 0.7T_c^F$ and (5) $T = 0.9T_c^F$, for the film thickness $p_0 d = 100$ and potential constants $d/a = 100$, $2mVa^2 = \pi^2$.

8. Comparison with experiment

In this section we compare our results with the experimental data [1–7]. We calculate the critical superflows for films with thicknesses and transition temperatures measured by Daunt *et al* [5]. We fit the potential $V(z)$ (2.3) in order to reproduce the measured transition temperature T_c^F for a given film. This procedure is single-valued. Next we find the critical superflow j_{Sc} as a function of temperature. The results obtained are drawn in figure 11. The values of j_{Sc} in our model are almost an order of magnitude higher than the measured ones [5]. Nevertheless, we have got a characteristic temperature dependence of the superflow:

$$j_{Sc} \propto (1 - T/T_c^F)^{3/2} \tag{8.1}$$

which is consistent with the experimental results [3, 5]. This relation holds for temperatures from $T \simeq 0.2T_c^F$ to $T = T_c^F$, i.e. almost in the entire range of temperature (see figure 11).

Next we calculate the critical superflows for films investigated by Xu and Crooker [2]. In figure 12 we draw the superfluid densities as a function of reduced temperature T/T_c^F. They are described by a universal curve (see figure 12). The superfluid density ρ_{Sc} is an order of magnitude higher than those measured by Xu and Crooker [2]. The conclusion is that there is a different mechanism responsible for strong suppression of the superflow in a thin film. However, the influence of the isolating ^{4}He layers on T_c^F [1, 4] and j_{Sc} [1, 4, 6, 7] can be partially explained by a change of the substrate field (see figures 3 and 7(*a*)). Since the presented microscopic model is quite general, other kinds of potential $V(z)$ cannot change the functions drawn in figures 11 and 12 significantly. A potential influences the results through the energy spectrum ϵ_ν (2.4). To reproduce a transition temperature T_c^F appropriate to the experiment, each kind of potential has to give nearly the same set of energies ϵ_ν (4.1) and cannot change the results. For this reason we do not discuss the applicability of the potentials used; even more realistic ones must give almost the same results.

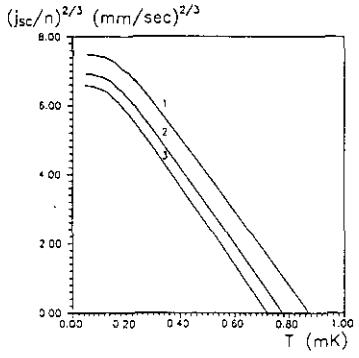

Figure 11. The superfluid density ρ_{Sc} versus the temperature T/T_c^F.

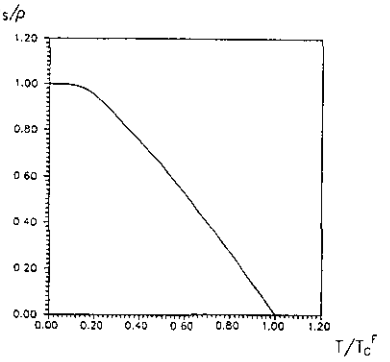

Figure 12. The critical superflow as a function of temperature for films with thickness d and critical temperature T_c^F: (1) $d = 1200$ Å, $T_c^F/T_c^B = 0.94$; (2) $d = 1100$ Å, $T_c^F/T_c^B = 0.84$; (3) $d = 1000$ Å, $T_c^F/T_c^B = 0.78$.

9. Conclusions

We have considered three superfluid two-dimensional states of ^{3}He in the presence of a superflow. The two-dimensional A (2-A) state is stabilized against the two-dimensional B (2-B) state by the superflow (figure 9). There is a phase transition from the 2-A state to the two-dimensional polar (2-P) state when the superfluid velocity increases (figure 5). The maximal superflow j_{Sc} is achieved in the 2-A state. For a wide range of temperature j_{Sc} is described by the power law (8.1), which is consistent with the theoretical results of Jacobsen and Smith [9] and Fetter and Ullah [8] in the Ginzburg–Landau limit. Our theoretical results are about an order of magnitude higher than the experimental ones. We have tried to explain the lowered superfluidity by the interaction of ^{3}He quasiparticles with the van der Waals-like field of the adsorbent. Whereas the effect of coating a substrate with ^{4}He [1, 4, 6, 7] can be partially explained by this model, the measured superflow values cannot be obtained. In experiments [1–7] the onset of dissipation occurs at relatively low superflows. This effect may be due to the very complex structure of the substrate; for instance, large-scale irregularities may cause the thinning effect of a film and lower the current. There are always uncertainties surrounding geometric characterization in these experiments. Some measurements [1, 4, 5] are performed in the U-tube geometry of the film-flow apparatus. Xu and Crooker [2] estimate that approximately the equivalent of 100 Å thick film is contained in scratches. This is also supported by the suggestion in [4] that the main influence of the substrate, rough or smooth, seems to be its influence on the film thickness. An additional mechanism limiting the critical current may be due to vortex creation and motion [4, 7]. This effect is expected to be strongly dependent on the substrate structure [26].

We have used several approximations in our method. The superfluid velocity v and the order parameter are assumed to be uniform in space [18]. Moreover, the gap function is two-dimensional, so the model is applicable rather to films with thickness $d \leqslant \xi_0$. We do not include the Fermi liquid forces, because we do not expect them to play a significant role compared to the influence of the substrate. As far as we know, there is no well defined Fermi liquid interaction in the proximity of a solid surface. It

should be added that the density of an adsorbed ^{3}He film is a function of distance from the substrate and in general is not constant, as assumed in our paper. These corrections to the model certainly will change the results. However, we do not believe that they will influence the calculated quantities substantially.

The theory presented here can be applied to thin films with more realistic and more complex potential of the substrate. This can be done by a suitable choice of the energy spectrum ϵ_ν (2.4).

In the following paper we analyse the effect of surface roughness on superflow and stability of the superfluid states studied in this paper.

Acknowledgments

One of us (GH) thanks Professor R E Packard for helpful comments on experiments with superfluid helium films as well as L S Borkowski and N Pavloff for valuable discussions.

References

[1] Steel S C, Zawadzki P, Harrison J P and Sachrajda A 1990 *Physica* B **165 & 166** 599
[2] Xu J and Crooker B C 1990 *Phys. Rev. Lett.* **65** 3005
[3] Davis J C, Amar A, Pekola J P and Packard R E 1988 *Phys. Rev. Lett.* **60** 302
[4] Harrison J P, Sachrajda A, Steel S C and Zawadzki P 1991 *Excitations in Two-Dimensional and Three-Dimensional Quantum Fluids* ed A G F Wyatt and H J Lauter (New York: Plenum) p 239
[5] Daunt J G, Harris-Lowe R F, Harrison J P, Sachrajda A, Steel S, Turkington R R and Zawadzki P 1988 *J. Low Temp. Phys.* **70** 547
[6] Freeman M R, Germain R S, Thuneberg E V and Richardson R C 1988 *Phys. Rev. Lett.* **60** 596
[7] Freeman M R and Richardson R C 1990 *Phys. Rev.* B **41** 11011
[8] Fetter A L and Ullah S 1988 *J. Low Temp. Phys.* **70** 515
[9] Jacobsen K W and Smith H 1987 *J. Low Temp. Phys.* **67** 83
[10] Harań G, Jacak L and Borkowski L S 1992 *Phys. Lett.* **165A** 165
[11] Tešanović Z and Valls O T 1986 *Phys. Rev.* B **33** 3139
[12] Harań G, Borkowski L and Jacak L 1990 *Physica* B **165 & 166** 679
[13] Krotscheck E, Saarela M and Epstein J L 1988 *Phys. Rev.* B **38** 111
[14] Pavloff N and Treiner J 1991 *J. Low Temp. Phys.* **83** 331
[15] Harań G, Jacak L and Borkowski L 1989 *Physica* B **159** 223
[16] Abrikosov A A, Gorkov L P and Dzyaloshinski I E 1975 *Methods of Quantum Field Theory in Statistical Physics* (New York: Dover)
[17] Jacak L 1989 *J. Phys.: Condens. Matter* **1** 3523
[18] Svidzinski A V 1982 *Space-Nonuniform Problems of Superconductivity Theory* (Moscow: Nauka) (in Russian)
[19] Jacak L 1981 *Acta Phys. Polon.* A **60** 205
[20] Volhardt D and Wölfle P 1990 *The Superfluid Phases of Helium 3* (Philadelphia: Taylor & Francis)
[21] Gonczarek R 1989 *Acta Phys. Polon.* A **76** 591
[22] Brusov P N and Popov V N 1981 *Zh. Eksp. Teor. Fiz.* **80** 1564
[23] Ambegaokar V, de Gennes P G and Rainer D 1974 *Phys. Rev.* A **9** 2676
[24] Leggett A J 1975 *Rev. Mod. Phys.* **47** 331
[25] Buchholtz L J 1990 *Physica* B **165 & 166** 657
[26] Ritchie D A, Saunders J and Brewer D F 1987 *Phys. Rev. Lett.* **59** 465